Glycoconj J (2014) 31:469–473
DOI 10.1007/s10719-014-9542-x

Flexibility and mutagenic resiliency of glycosyltransferases

Marie Lund Bay · Jose A. Cuesta-Seijo · Joel T. Weadge · Mattias Persson · Monica M. Palcic

Published online: 13 August 2014

Abstract The human blood group A and B antigens are synthesized by two highly homologous enzymes, glycosyltransferase A (GTA) and glycosyltransferase B (GTB), respectively. These enzymes catalyze the transfer of either GalNAc or Gal from their corresponding UDP-donors to αFuc1–2βGal-R terminating acceptors. GTA and GTB differ at only four of 354 amino acids (R176G, G235S, L266M, G268A), which alter the donor specificity from UDP-GalNAc to UDP-Gal. Blood type O individuals synthesize truncated or non-functional enzymes. The cloning, crystallization and X-ray structure elucidations for GTA and GTB have revealed key residues responsible for donor discrimination and acceptor binding. Structural studies suggest that numerous conformational changes occur during the catalytic cycle. Over 300 ABO alleles are tabulated in the blood group antigen mutation database (BGMUT) that provides a framework for structure-function studies. Natural mutations are found in all regions of GTA and GTB from the active site, flexible loops, stem region and surfaces remote from the active site. Our characterizations of natural mutants near a flexible loop (V175M), on a remote surface site (P156L), in the metal binding motif (M212V) and near the acceptor binding site (L232P) demonstrate the resiliency of GTA and GTB to mutagenesis.

Keywords Blood group glycosyltransferases · Natural mutations

Abbreviations

GTA Blood group A synthesizing $\alpha-1,3$-*N*-acetygalactosaminyltransferase
GTB Blood group B synthesizing α-1,3-galactosyltransferase

M. L. Bay · J. A. Cuesta-Seijo · J. T. Weadge · M. Persson · M. M. Palcic (✉)
Carlsberg Laboratory, Gamle Carlsberg Vej 10,
DK-1799 Copenhagen V, Denmark
e-mail: monicapalcic@gmail.com

Introduction

Glycosyltransferases catalyze the transfer of a glycosyl residue from donor substrates typically nucleotide sugars, to a wide variety of acceptors [1, 2]. Acceptors include saccharides, proteins, lipids, DNA, natural products and unnatural compounds. Glycosyltransferases are encoded by about 1–2 % of all genes sequenced to date. Currently over 140,000 gene sequences for glycosyltransferases are tabulated in the CAZy GT database (www.cazy.org) [3],though the activities of only about 2–3 % have been biochemically verified. In contrast to the diversity of structural folds seen for glycosidases, the nucleotide donor utilizing GTs characterized to date exhibit variants of only two structural fold types: the GT-A-fold and the GT-B-fold [1, 2].

The human blood group A and B antigen synthesizing enzymes GTA and GTB are ideal models for investigating the mechanism and structure-function relationships for retaining glycosyltransferases of the GT-A-fold type. GTA is an α-1,3-*N*-acetygalactosaminyltransferase which transfers GalNAc from UDP-GalNAc donor to αFuc1–2βGal-R terminating acceptors producing blood group A antigens (Fig. 1). GTB is an α-1,3-*N*-galactosyltransferase transferring Gal from UDP-Gal to αFuc1–2βGal-R acceptors producing blood group B antigens (Fig. 1). GTA and GTB are the most homologous of all glycosyltransferases since they differ by only 4 amino acids of 354 in their full length sequences [4]. These four residues are Arg/Gly-176, Gly/Ser-235, Leu/Met-266 and Gly/Ala-268 in GTA and GTB, respectively [4]. Two of these four amino acids Leu/Met-266 and Gly/Ala-268 have been suggested to determine donor specificity [5]. Gly/Ser-235 and Leu/Met-266 are believed to affect acceptor binding [6]. Crystal structures of GTA and GTB in complex with their substrates reveal details of substrate binding interactions and suggest that numerous conformational changes occur during catalysis [7] which can be exploited for inhibitor design [8]. Over 300 ABO alleles are tabulated in the blood group antigen mutation database (BGMUT) [9] that provides a framework

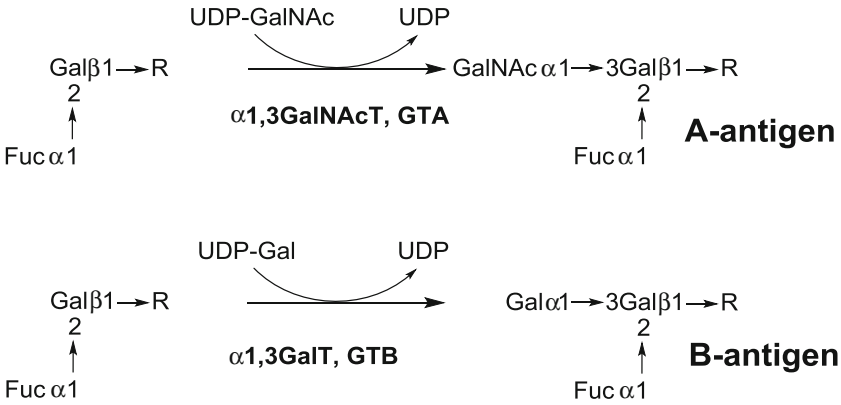

Fig. 1 The reactions catalyzed by the human blood group A and B synthesizing enzymes

for structure-function studies. Natural mutations are found in all regions of GTA and GTB from the active site, flexible loops that undergo conformational changes during catalysis, stem regions and surfaces remote from the active site. In this study, we report our characterizations of naturally occurring mutations near the internal flexible loop (V175M) and acceptor binding site (L232P), on a remote surface site (P156L) and in the metal binding motif (M212V) (Fig. 2) which demonstrate the resiliency of GTA and GTB to mutagenesis.

Experimental procedures

Cloning and expression

The mutant enzymes were cloned and expressed in *E. coli* using standard site-directed mutagenesis with a QuikChange II XL Site-Directed Mutagenesis Kit (Stratagene). Plasmid vector pCWΔlac containing either GTA or GTB genes (amino acids 63–354) which are codon optimized for expression in *E. coli* was used as a template. The PCR cycling conditions were: Initial denaturation at 95 °C for 35 s followed by 18 cycles at 95 °C for 30s, 60 °C for 60s, 68 °C for 10 min and a final extension at 68 °C for 10 min. The primers used for mutagenesis were as follows:

P156L forward5'-CACCGACCAGCTGGCCGCGGTTC-3'

P156Lreverse5'-GAACCGCGGCCAGCTGGTCGGTG-3'

V175Mforward5'CTGTCCGTTCTGGAAATGGGCGCCTACAAAC-3'

V175M reverse5'-GTTTGTAGGCGCCCATTTCCAGAACGGACAG-3'

M212V forward 5'-CCTGGTTTGCGTTGACATGGACATGGAGTTCCGTG-3'

M212V reverse 5'-CACGGAACTCCATGTCCATGTCAACGCAAACCAGG-3'

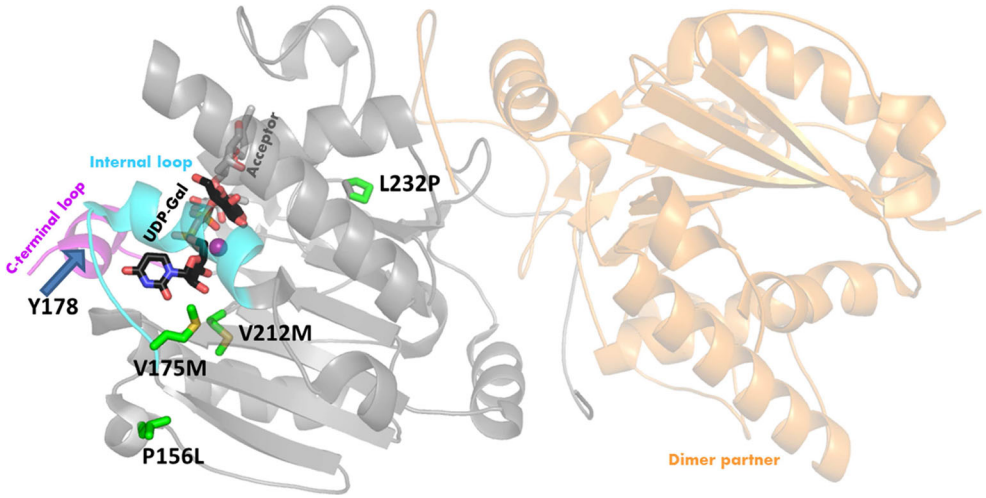

Fig. 2 Overview of a GTB enzyme in the closed conformation with bound substrates, depicted with gray transparent ribbons, and the position of the described mutants. GTB is a dimer *in-vivo*, the second monomer is depicted in pale orange ribbons. The 4 mutants are highlighted (side chains only) with green carbons. The internal loop (residues 175–191) is depicted in cyan, and the C-terminal loop (from residue 346) in purple. Also highlighted are the UDP-Gal donor (black carbons, stick model), the manganese atom (purple sphere) and the acceptor (*gray carbons, stick model*) and Y178 (*arrow*) within the cyan part of the ribbon

L232P forward5'-CGCTGTTCGGTACCCCGCACCC GAGCTTCTAC-3'

L232P reverse5'-GTAGAAGCTCGGGTGCGGGGTA CCGAACAGCG-3'

The altered nucleotides are underlined. To digest template methylated non-mutated plasmid DNA the PCR reaction mixture was treated with 1 μl *Dpn*I (10 U/μl) for 60 min at 37 °C. The *Dpn*I treated plasmids were transformed into *E.coli* XL10-Gold cells and sequencing was performed by Agowa (Berlin, Germany). Positive mutants were transformed into *E.coli* BL21-Gold cells for expression.

Purification –Enzymes were produced from the respective clones, purified by ion-exchange (SP-Sepharose FF) and affinity chromatography (UDP-hexanolamine Sepharose eluted with 4–10 mM UDP) as previously described [10].

Enzyme kinetics Kinetic constants were determined with a radiochemical assay using α-l-Fuc*p*-(1→2)-β-D-Gal*p*-O-$(CH_2)_7CH_3$ as an acceptor [11]. In this assay, a Sep-Pak reverse-phase cartridge is used to isolate hydrophobic radiolabeled products from unreacted donor. Assays were carried out at 37 °C in a total volume of 12 μl in 50 mM MOPS buffer, pH 7.0, 20 mM $MnCl_2$ and BSA (1 mg/ml). At least six different concentrations of donor and acceptor were employed. Reactions were terminated by dilution with 500 μl water, then the mixture was transferred to a Sep-Pak cartridge which was washed with 100–200 ml water to remove unreacted donor. Radiolabeled hydrophobic product was eluted from the cartridge into a scintillation vial with 5 ml methanol then counted in a Beckman LS6500 counter after addition of 10 ml of Ecolite cocktail. Initial rate conditions were linear with no more than 10-20 % of the substrate consumed in the reaction. For the donors, the K_m values were determined at 1.0 mM acceptor and the K_m for the acceptor was determined at 1.0 mM donor. The kinetic parameters k_{cat} and K_m were obtained by non-linear regression analysis of the Michaelis Menten equation with the Graph Pad PRISM 3.0 program (GraphPad Software, San Diego, CA). Enzyme concentrations were determined using the Bradford method using bovine gamma globulin as a protein standard.

Modelling of mutant enzymes

Modeling of the mutants was made by modifying structure PDB_ID: 2RJ7 which is a dual specificity hybrid AABB enzyme with the following four critical residues Arg-176, Gly-235, Met-266 and Ala-268 [7]. This structure features bound UDP-Gal donor andα-L-Fuc*p*-(1→2)-β-D-Gal*p*-O-$(CH_2)_7CH_3$acceptor with the enzyme in a fully closed conformation comprised of a structured internal loop and a structured C-terminus. Amino acid mutations were made by changing their side chains into their most likely conformer of the new residue with PyMOL (PyMOL Molecular Graphics System, Version 1.5.0.4 Schrödinger, LLC). In cases where this resulted in clashes, further manual adjustment of individual atoms was carried out with PyMOL until clashes were absent. Figures showing the mutations were also rendered with PyMOL

Results and discussion

The mutant enzymes all expressed well as soluble proteins and were purified to homogeneity from 1 L of *E. coli* culture. The quantities of isolated enzymes were 25 mg/L GTB-P156L, 36 mg/L GTA-P156L, 2 mg/LGTB-V175M,18 mg/L GTA-V212M and16mg/L GTB-L232P. The lower quantity of purified GTB-V175M is due to somewhat weaker binding of the enzyme to the UDP-hexanolamine column which resulted in the loss of 10 mg of enzyme in the column washing steps.

The K_m and k_{cat} values for UDP-GalNAc or UDP-Gal donor and α-Fuc*p*-(1→2)-β-Gal*p*-O-$(CH_2)_7$-CH_3 acceptor with GTA and GTB have previously been reported [12] and are given in Table 1. The P156L mutation has different effects on GTA and GTB. The k_{cat} for GTA-P156L is 34 % that of GTA (Table 1). For GTA-P156L the K_m for UDP-GalNAc donor is increased two-fold compared to GTA. In contrast, for GTB-P156L there is no effect on the k_{cat} and the K_m for donor increased 1.5-fold compared to GTB. There is no effect on the K_m for the acceptor for either mutant.

The GTB-V175M mutation resulted in a reduction in k_{cat} and K_m for acceptor with little effect on the donor Km. The latter is surprising since there was a decrease in the binding of this mutant enzyme to the UDP-hexanolamine column suggesting donor binding might be impaired. The GTA-V212M mutation which is in the metal binding motif has surprisingly

Table 1 Kinetic parameters for GTA, GTB and naturally occurring mutant enzymes

Enzyme	UDP-GalNAc			UDP-Gal		
	K_A[a]	K_B[b]	k_{cat} (s^{-1})	K_A	K_B	k_{cat} (s^{-1})
GTA[c] GTB[c]	9.9	8.7	17.5	88	27	5.1
GTA-P156L GTB-P156L	8[d]	20	6	87	41	5.2
GTB-V175M				38	26	3
GTA-V212M	34	85	17			
GTB-L232P				500	24	2

[a] K_m for the acceptor in μM

[b] K_m for the donor in μM

[c] Data from reference 12

[d] The errors on Km values are typically 10–15 % and k_{cat} 5–15 %

little effect on k_{cat}, while there are increases in the Km's for donor and acceptor. For the GTB-L232P mutation there was a great elevation in the Km for acceptor with substrate inhibition at concentrations greater than 1.5 mM acceptor. There was no effect on donor binding while the k_{cat} was also greatly reduced.

To understand the potential effects of the mutations on catalysis, the respective mutants were modeled onto a GTB structure (Fig. 2). This structure shows the enzyme in a closed conformation with UDP-Gal donor and acceptor substrates bound to the enzyme. Two loops are shown in cyan (internal loop) and purple (C-terminal residues). In the absence of substrates, the C-terminal loop is disordered while the internal loop is disordered or in a semi-closed conformation with an unusual distorted helical structure [7]. The P156L mutation appears to be remote from the active site where substrates are bound (Fig. 2). In Fig. 3, it can be seen that P156L caps a helix that directly interacts with the end of the internal flexible loop (in cyan). The internal loop is flexible and changes from a distorted kinked helical structure with loss of a hydrogen bond between Y178 (arrow, Fig. 2) and E190 in going from the semi-closed (kinked helix) to the closed conformation with the helix as shown in cyan. Thus mutations of P156 can be expected to affect the dynamics of the internal loop folding which can account for the elevation of K_m for UDP-GalNAc and decrease in k_{cat} seen in the GTA-P156L mutant. For GTB-P156L there was also an elevation in K_m for UDP-Gal with no reduction in k_{cat} suggesting the loop folding dynamics were not as drastically affected in GTB. Since GTB has a small flexible Gly176 as a critical residue in this loop folding region while GTA has Arg176, it is predicted to be more resilient to mutations that affect loop folding dynamics.

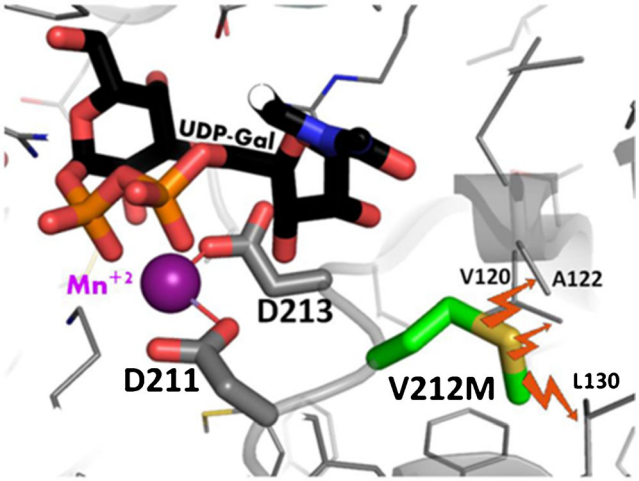

Fig. 4 Details around V212M (*green carbons*). The donor molecule (*black carbons, stick model*), the manganese ion (purple sphere) and the aspartates in the $D_{211}XD_{213}$ metal binding motif (*grey carbons, stick model*) are also highlighted in the picture. The methionine side chain in the V212 mutant is too large to fit in the pocket defined by V120, A122 and L130. Likely clashes with these residues are depicted with bent arrows. This should result in a displacement of the whole DXD motif and interference with the binding of manganese

For GTB-V175M, the dynamics of internal loop folding should also be affected (Fig. 3). However, in this case the only effect was on turnover with a reduction in k_{cat} rather than substrate K_ms. This enzyme exhibited somewhat weaker binding to the UDP-hexanolamine column than the other mutants, and GTA and GTB since much of it eluted in the column washing step during purification, suggesting there is some effect on UDP recognitionin GTB-V175M.

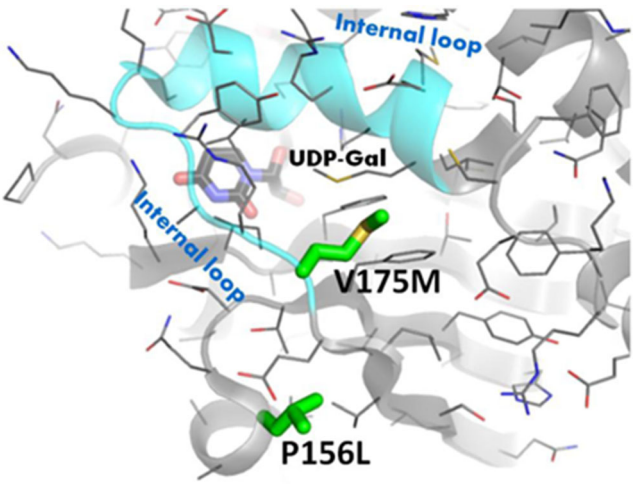

Fig. 3 Zoom into the P156L and V175M mutants, highlighted with green carbons. The internal loop is highlighted with a cyan ribbon and the donor (*stick model, black carbons*) is visible in the back. V175M sits at the hinge point for movement of the internal loop, while P156L caps a helix that directly interacts with the loop. It is likely that both mutations affect the dynamics of internal loop folding

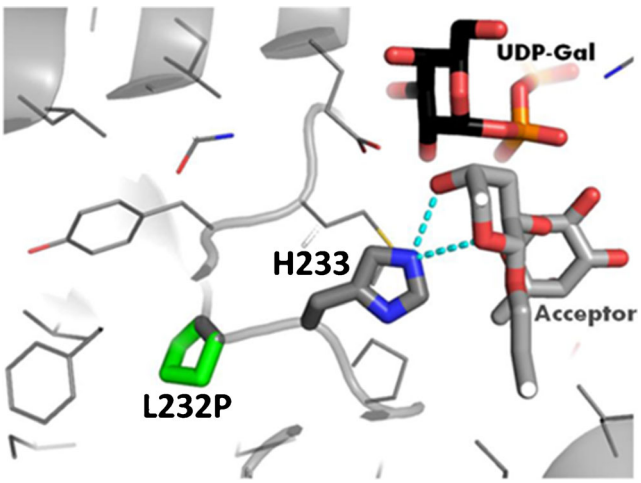

Fig. 5 Details around the L232P mutation (*green carbons*). This residue is adjacent to His233 (*stick model, gray carbons*) which should be displaced as a result of the mutation. His233 is hydrogen bonded (*dashed cyan lines*) to the acceptor molecule (*gray and red stick model to the right*), and the geometry of this interaction should be affected as a consequence of the L232P mutation. The donor (*stick model, black carbons*) is also visible

The GTA-M212V mutation is modeled in Fig. 4. It occurs in the middle of the DXD metal binding motif and was expected to have a dramatic effect on catalysis since there is no room to accommodate the bulky methionine in the hydrophobic pocket formed by Val120, Ala122 and Leu130. The methionine was predicted to displace the DXD motif and disturb the position of the Mn^{2+} ion [13]. While acceptor and donor binding were both affected with elevations in K_m, there was no effect on k_{cat}. This suggests some flexibility in the metal binding region that can accommodate the bulky methionine that is not evident in X-ray structures.

The GTB-L232P mutation is modeled in Fig. 5. This residue is next to His233 which is hydrogen bonded to the acceptor. The proline mutation is predicted to displace His233 which should affect acceptor binding which can account for the elevation in Km for acceptor. Donor binding and turnover are not affected. Taken together, these mutations along with previous mutations [7, 12, 13] demonstrate conformational flexibility in GTA and GTB enzymes that confer resiliency to mutagenesis. This flexibility is being investigated by normal mode analysis to gain better insights into the dynamics of GTA and GTB conformational transitions.

Acknowledgments This study was funded in part by a grant from FNU to M.M.P. Mette Bien is thanked for assistance with the characterization of the V212mutant.

References

1. Lairson, L.L., Henrissat, B., Davies, G.J., Withers, S.G.: Glycosyltransferases: structures, functions and mechanisms. Annu. Rev. Biochem. **77**, 521–555 (2008)
2. Breton, C., Fournel-Gigleux, S.: Palcic, M.M.: Recent structures, evolution and mechanisms of glycosyltransferases. Curr. Opin. Struct. Biol. **22**, 540–549 (2012)
3. Lombard, V., Ramulu, H.G., Drula, E., Coutinho, P.M., Henrissat, B.: The carbohydrate-active enzymes database (CAZy) in 2013. Nucleic Acids Res. **42**, 490–495 (2014)
4. Yamamoto, F., Clausen, H., White, T., Marken, J., Hakomori, S.: Molecular and genetic basis of the histo-blood group ABO system. Nature **345**, 229–233 (1990)
5. Patenaude, S.I., Seto, N.O.L., Borisova, S.N., Szpacenko, A., Marcus, S.L., Palcic, M.M., Evans, S.V.: The structural basis for specificity in human ABO(H) blood group biosynthesis Nature. Struct. Biol. **9**, 685–690 (2002)
6. Letts, J.A., Rose, N.L., Fang, Y.R., Barry, C.H., Borisova, S.N., Seto, N.O.L., Palcic, M.M., Evans, S.V.: Differential recognition of the type I and II H-antigen acceptors by the human ABO (H) blood group A and B glycosyltransferases. J. Biol. Chem. **281**, 3625–3632 (2006)
7. Alfaro, J.A., Zheng, R.B., Persson, M., Letts, J.A., Polakowski, R., Bai, Y., Borisova, S.N., Seto, N.O.L., Lowary, T.L., Palcic, M.M., Evans, S.V.: ABO (H) blood group A and B glycosyltransferases recognize substrate *via* specific conformational changes. J. Biol. Chem. **283**, 10097–100108 (2008)
8. Jørgensen, R., Pesnot, T., Lee, H.J., Palcic, M.M., Wagner, G.K.: Base-modified donor analogues reveal novel dynamic features of a glycosyltransferase. J. Biol. Chem. **288**, 26201–26208 (2013)
9. Patnaik, S.K., Helmberg, W., Blumenfeld, O.O.: BGMUT: NCBI dbRBC database of allelic variations of genes encoding antigens of blood group systems. Nucleic Acids Res. **40**, D1023–D1029 (2012)
10. Seto, N.O.L., Compston, C.A., Szpacenko, A., Palcic, M.M.: Enzymatic synthesis of blood group A and B trisaccharide analogues. Carbohydr. Res. **324**, 161–169 (2000)
11. Palcic, M.M., Heerze, L.D., Pierce, M., Hindsgaul, O.: The use of hydrophobic synthetic glycosides as acceptors in glycosyltransferase assays. Glycoconj. J. **5**, 49–63 (1988)
12. Marcus, S.L., Polakowski, R., Seto, N.O.L., Leinala, E., Borisova, S.N., Blancher, A., Roubinet, F., Evans, S.V., Palcic, M.M.: A single point mutation reverses the donor specificity of human blood group B-synthesizing galactosyltransferase. J. Biol. Chem. **278**, 12403–12405 (2003)
13. Hult, A.K., Yazer, M.H., Jørgensen, R., Hellberg, A., Hustinx, H., Peyrard, T., Palcic, M.M., Olsson, M.L.: Weak A phenotypes associated with novel ABO alleles carrying the A^2-related 1061C deletion and various missense substitutions. Transfusion **50**, 1471–1486 (2010)